

## INTRODUCTION

The Star Formation History of the universe earlier than  $z \sim 4$  is under explored in the Far IR. Throughout the majority of the universe's history, dust obscuration has patterned the majority of star formation only visible in the far IR, it is uncertain how this pattern will hold up in the early universe, due to dependence on models of dust formation in early galaxies. So the only way to get a full picture of the star formation history, and therefore the evolution of the universe, is to observe the star formation rates of the early galaxies in long wavelengths. SuperSpec will enable this by providing a large instantaneous bandwidth spectrometer to assign a redshift to the observed galaxies and observe the [C II] emission line, which is a very bright IR emission line that acts as a tracer for star formation. SuperSpec additionally paves the way for future multi-pixel instruments for multi-object spectrometers and Line Intensity Mapping by implementing a mm-wave spectrometer on a  $\sim 20 \text{ cm}^2$  silicon die. A several order of magnitude reduction in size compared to the previous generations of comparable grating spectrometers.

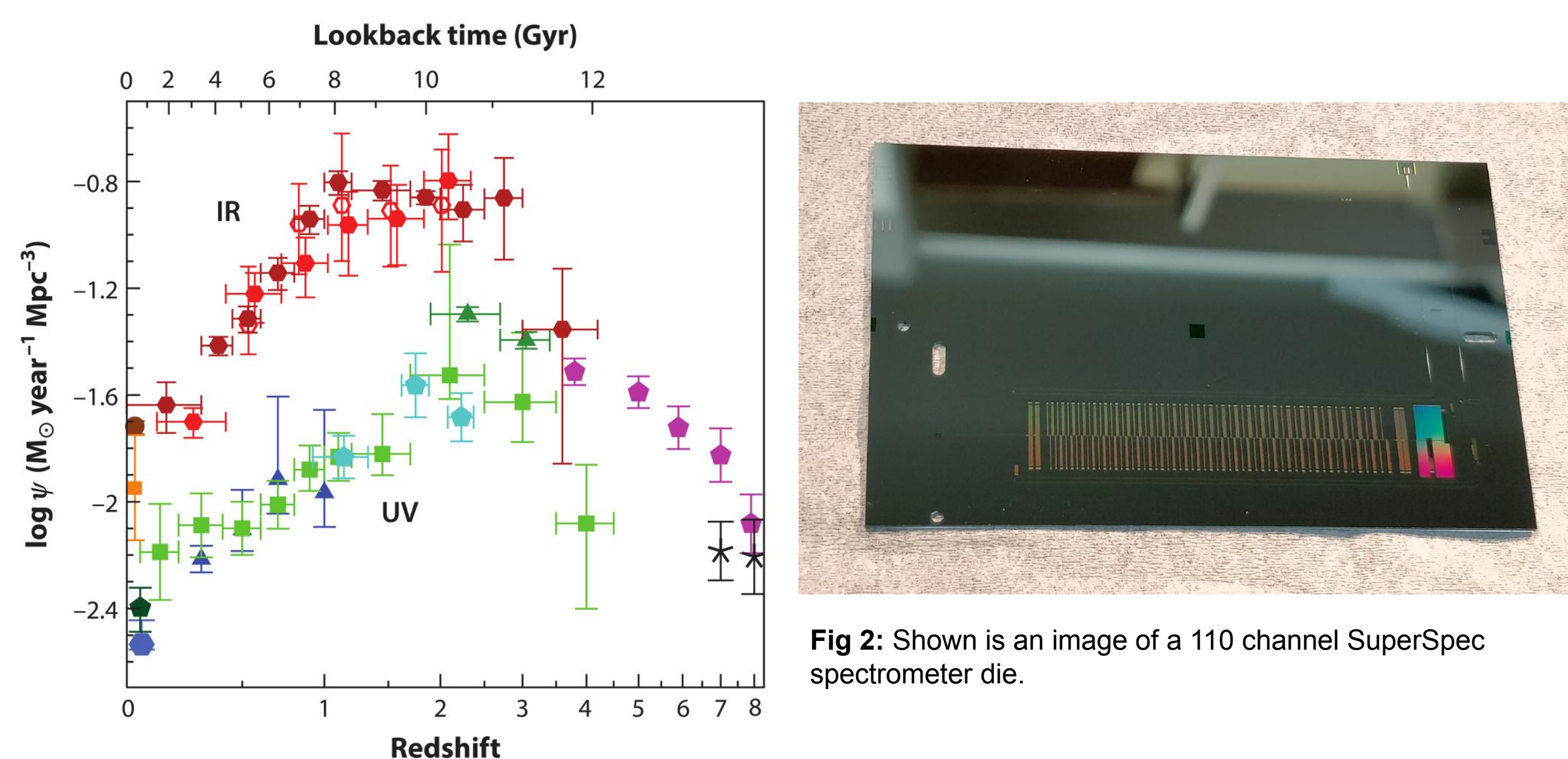


Fig 2: Shown is an image of a 110 channel SuperSpec spectrometer die.

Fig 1: Originally from Madau & Dickinson 2014 [2]. The observed star formation rate of the universe in both the UV and IR, noting the lack of IR data at  $Z > 4$

## FILTERBANKS

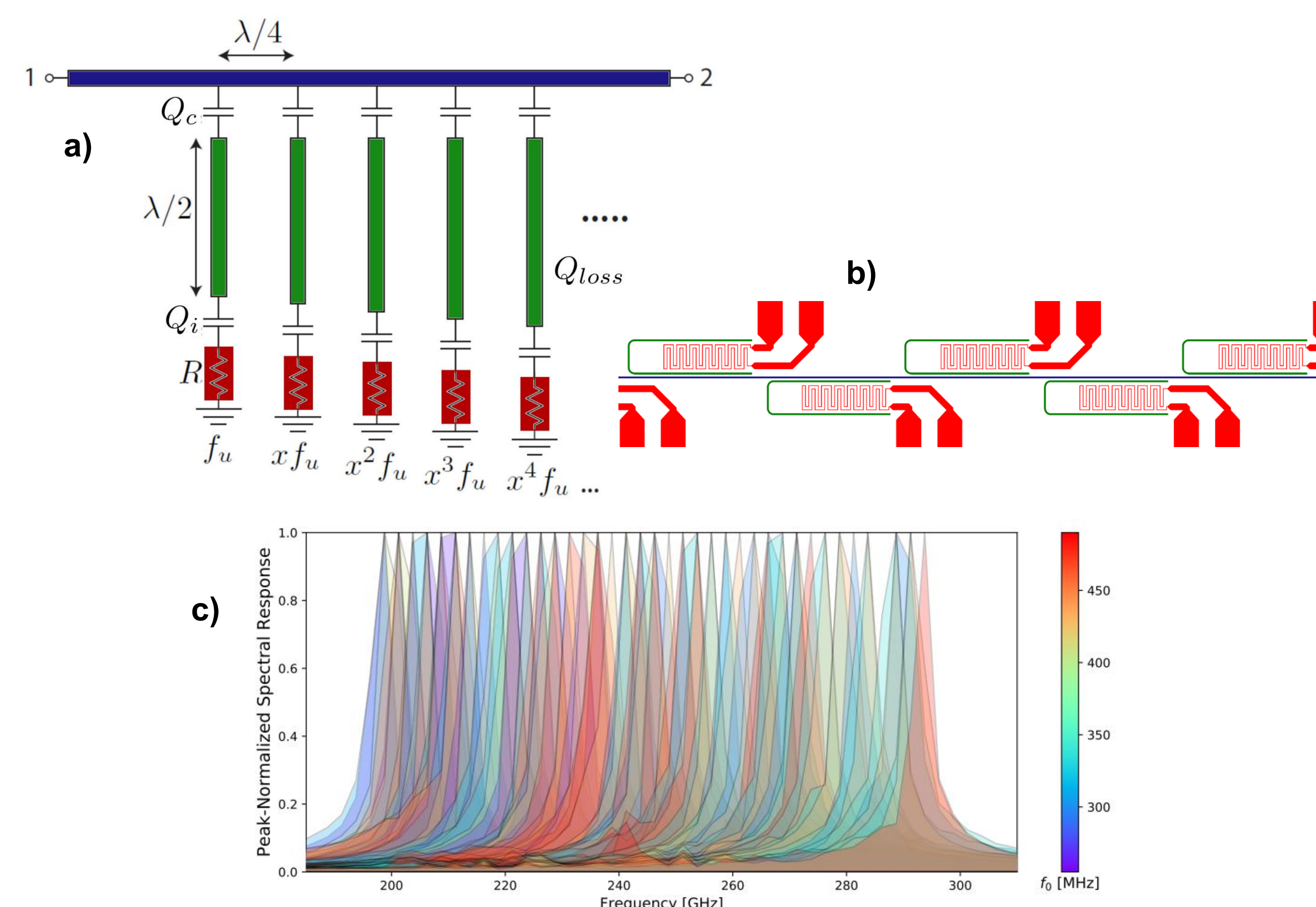


Fig 8: a) A circuit representation of the SuperSpec filterbank design. A series of half-wave resonators are capacitively coupled to a microstrip line carrying the incident radiation and act as a filter to transmit the radiation at its resonance to the detector, shown as a resistor since it is an absorbing element. b) An image of the circuit filterbank layout color coded with the corresponding colors for each element. c) A measured filterbank response of a full band 110 channel device measured with 1GHz resolution by K. Karkare, peak normalized.

SuperSpec uses a filterbank constructed with mm-wave half wavelength resonators acting as a filter to mediate the coupling of radiation from a microstrip feedline and a kinetic inductance detector (KID) and its channel resolution set by the mm-wave Q. This allows a compact, frequency multiplexed spectrometer on a single silicon die. Additionally, the mm-wave resonators are spaced by an odd multiple of quarter wavelengths so that the reflections of adjacent resonators destructively cancel. This causes a resonant condition that further enhances the absorption of the filterbank, but asymmetrical channel profiles in frequency. Design work and optimization of the coupling parameters makes use of the python-based modeling approach outlined in [3] by G. Che.

## DEVICE DESIGN

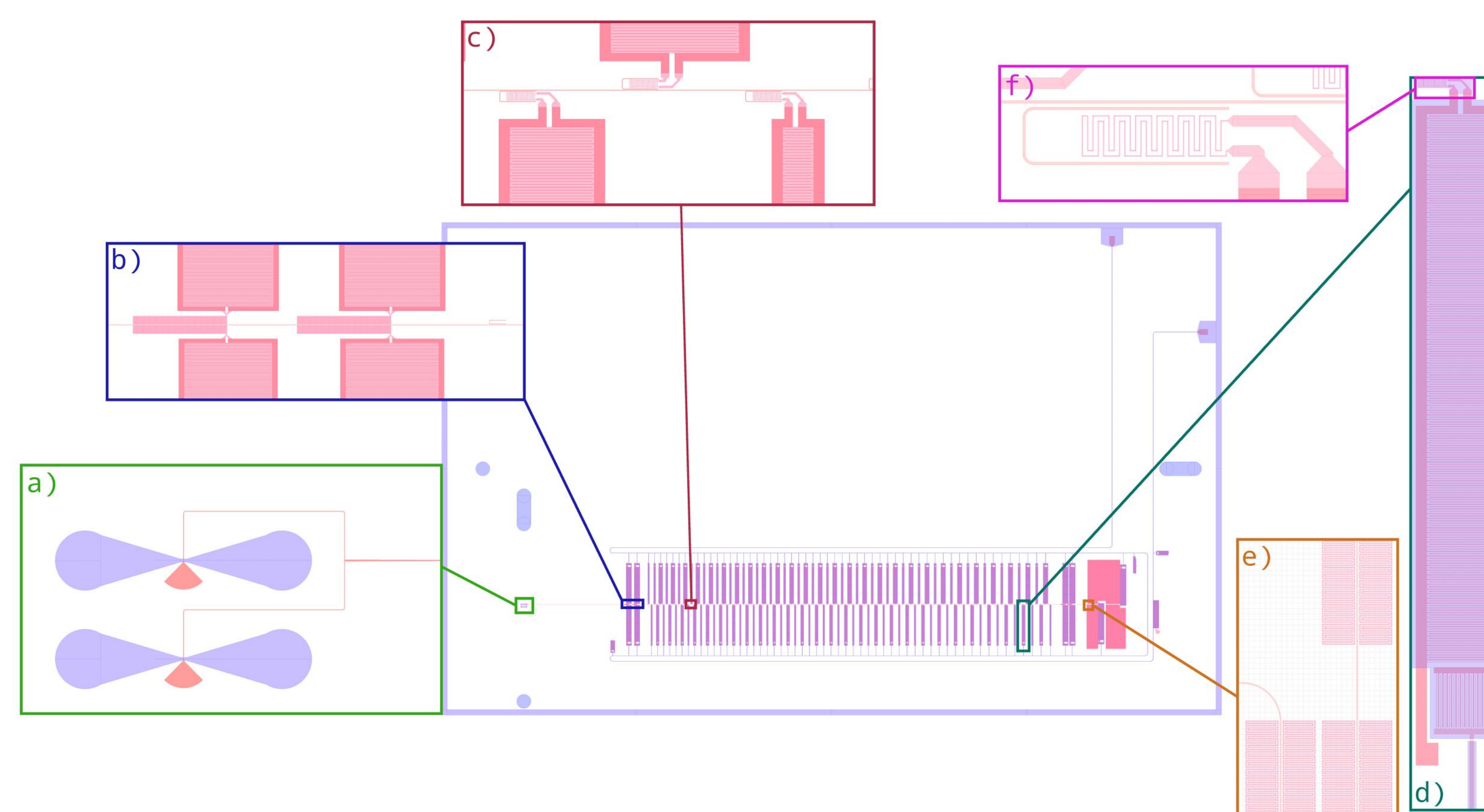


Fig. 3: The die layout of the devices for SuperSpec demonstration at the Large Millimeter Telescope (LMT). The device is lens coupled using a flared twin-slot antenna and a die mounted AR-coated TiN lens to get the incident light onto a microstrip (a). The light then propagates to the feed bank, first encountering broadband detectors (b) for testing and calibration which is a KID coupled to the radiation, without a half-wave filter. The main filterbank (c) consists of a series of mm-wave  $\lambda/2$  resonators arrayed along the feedline with the  $\lambda/2$  resonator wrapped around the inductor of the KID detector. The microstrip feedline terminates after snaking through TiN meanders (e) to absorb any remaining radiation and prevent reflections and standing waves. The filterbank KIDs are shown in (d) with the readout coupling capacitors on the bottom, with the majority of the area taken up by the main interdigitated capacitor to form the LC resonance and set the readout frequency. The inductor is a meandering TiN trace that has a very small volume ( $2.6 \mu\text{m}^3$ ), shown in (f).

Above, is the layout of the device that will be used in the SuperSpec on-sky demonstration. The device will cover much of the 1mm atmospheric window, with the filterbank spanning the 200-300 GHz frequency range with a resolution of  $R \sim 270$ . There are 110 KID detector channels all readout with the same readout line, with resonances between 200-450MHz. The compact size of the capacitors, despite the small volume of inductors, is due both to the high normal state sheet resistance of TiN ( $\sim 50 \Omega/\square$ ) and the increased readout frequency on the low end (200 MHz as opposed to the 100MHz resonators in previous designs shown at the last conference).

## LMT PROJECTED PERFORMANCE

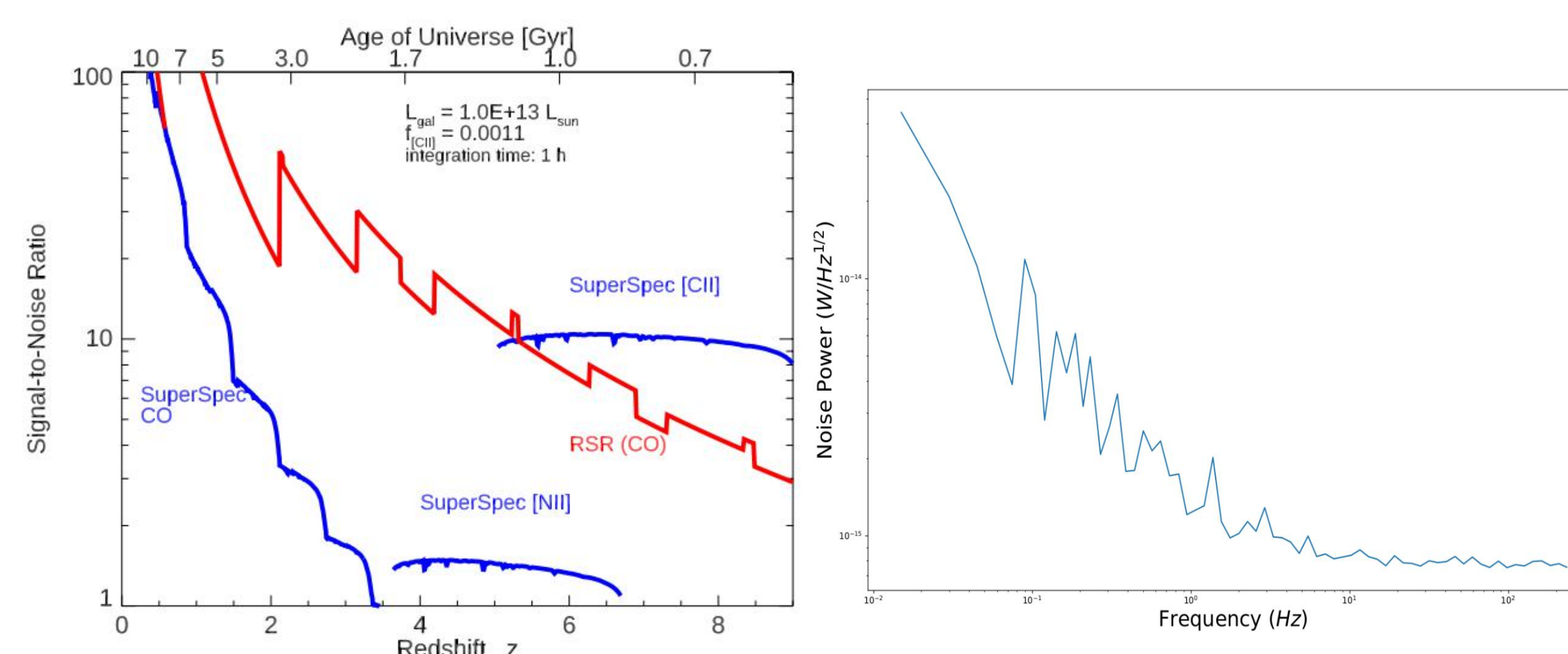


Fig 7: Left, Projected sensitivity of SuperSpec on LMT detecting various emission lines including [C II], [N II], and the CO ladder in a  $10^{13}$  Solar Luminosity galaxy, with 1 hr of integration time. For comparison, the Redshift Search Receiver (RSR) sensitivity observing the CO ladder on the LMT is shown under similar observing conditions. Right, The noise equivalent power (NEP) of a sample resonator of a deployment candidate die, with a  $\sim 50 \text{ k}\Omega$  load and in the cryostat, as it will likely be deployed. The observed performance is being used to inform the plot on the left.

SuperSpec has previously demonstrated good performance with its  $2.6 \mu\text{m}^3$  small volume TiN inductors at the cryostat operating temperatures in previous prototype dies. We have previously achieved detectors with NEPs of  $3 * 10^{-18} \text{ W}/\sqrt{\text{Hz}}$  at our cryostats operating temperature of 220mK, enough for background limited observation, and NEPs as low as  $7 * 10^{-19} \text{ W}/\sqrt{\text{Hz}}$  at colder temperatures ( $< 130 \text{ mK}$ ) with previous 50 channel prototypes [4]. Our full-band devices demonstrate single channel NEP, with reference to input power to the full instrument, near  $\sim 7 * 10^{-16} \text{ W}/\sqrt{\text{Hz}}$ , noting that we will have a chopping mirror able to modulate the signal up to 3Hz. This performance points to some yet undiagnosed optical loss, but will still allow for the detection of [C II] lines of a HyLIRG or brighter ULIRG galaxy within less than an hour on the telescope. Troubleshooting fabrication issues and diagnosing the optical loss should allow significant further improvement of SuperSpec detection sensitivity in the near future.

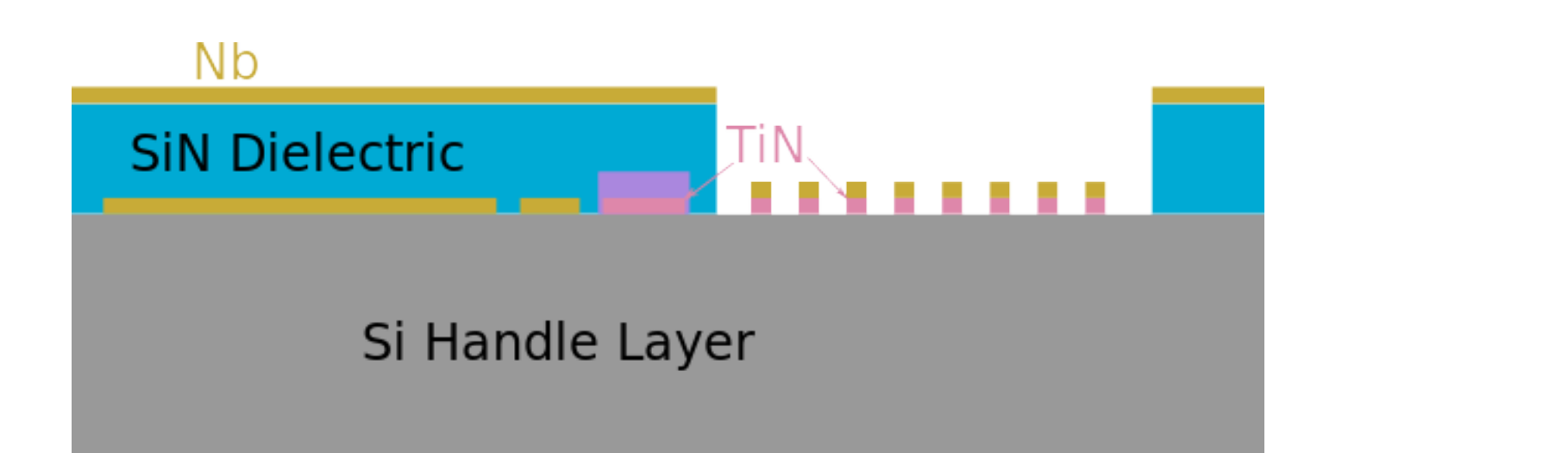


Fig 4: The cross section of layers on a SuperSpec die. SuperSpec is using an inverted Nb microstrip with a SiN dielectric. A 25nm thick TiN layer is patterned into the KIDS resonators, with the non-inductor parts of the KIDs also covered with Nb to remove non-sensing inductance. Additionally, to prevent a large parasitic capacitance to ground and extra TLS noise, the ground plane and dielectric is etched away above the KID capacitors.

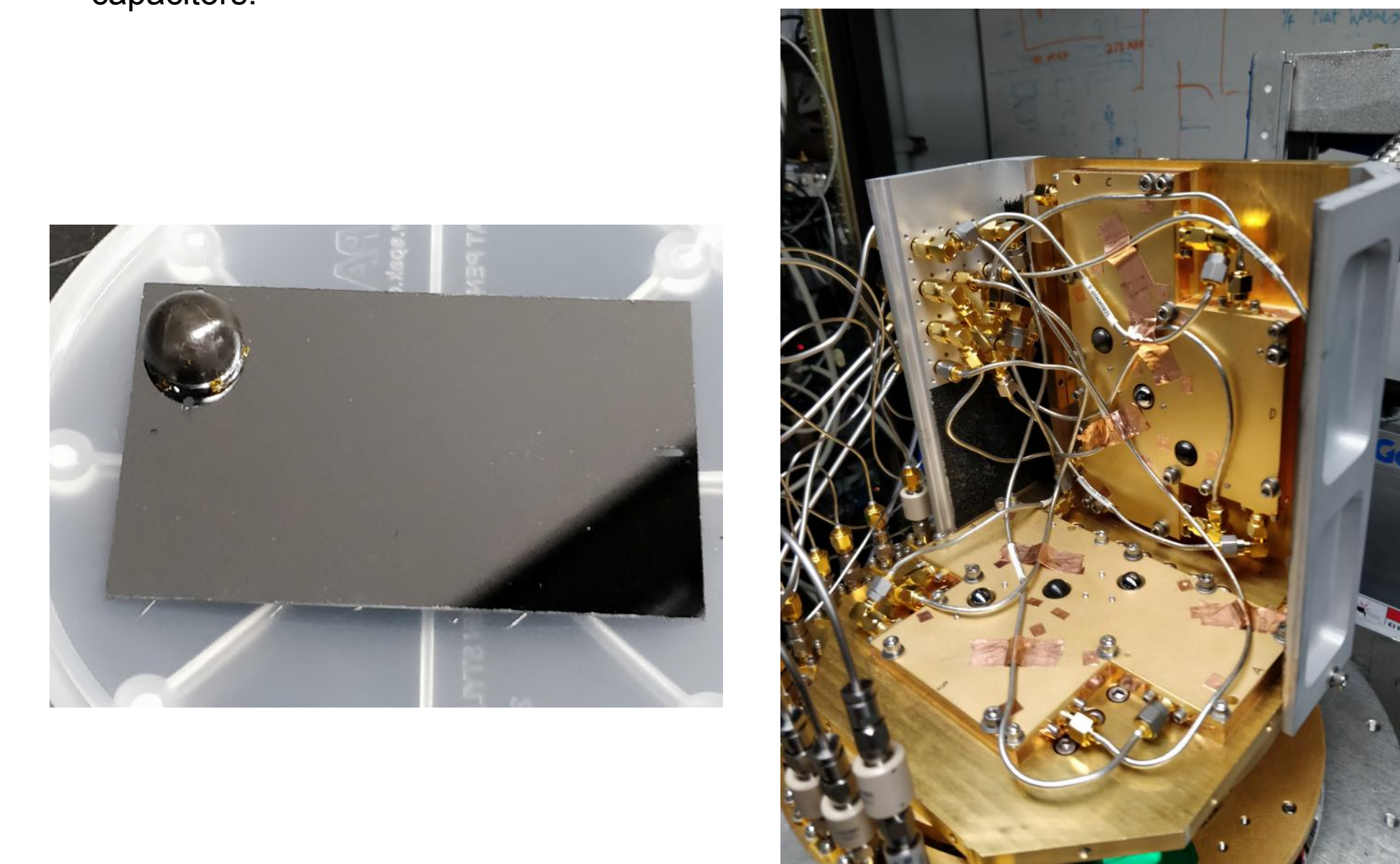
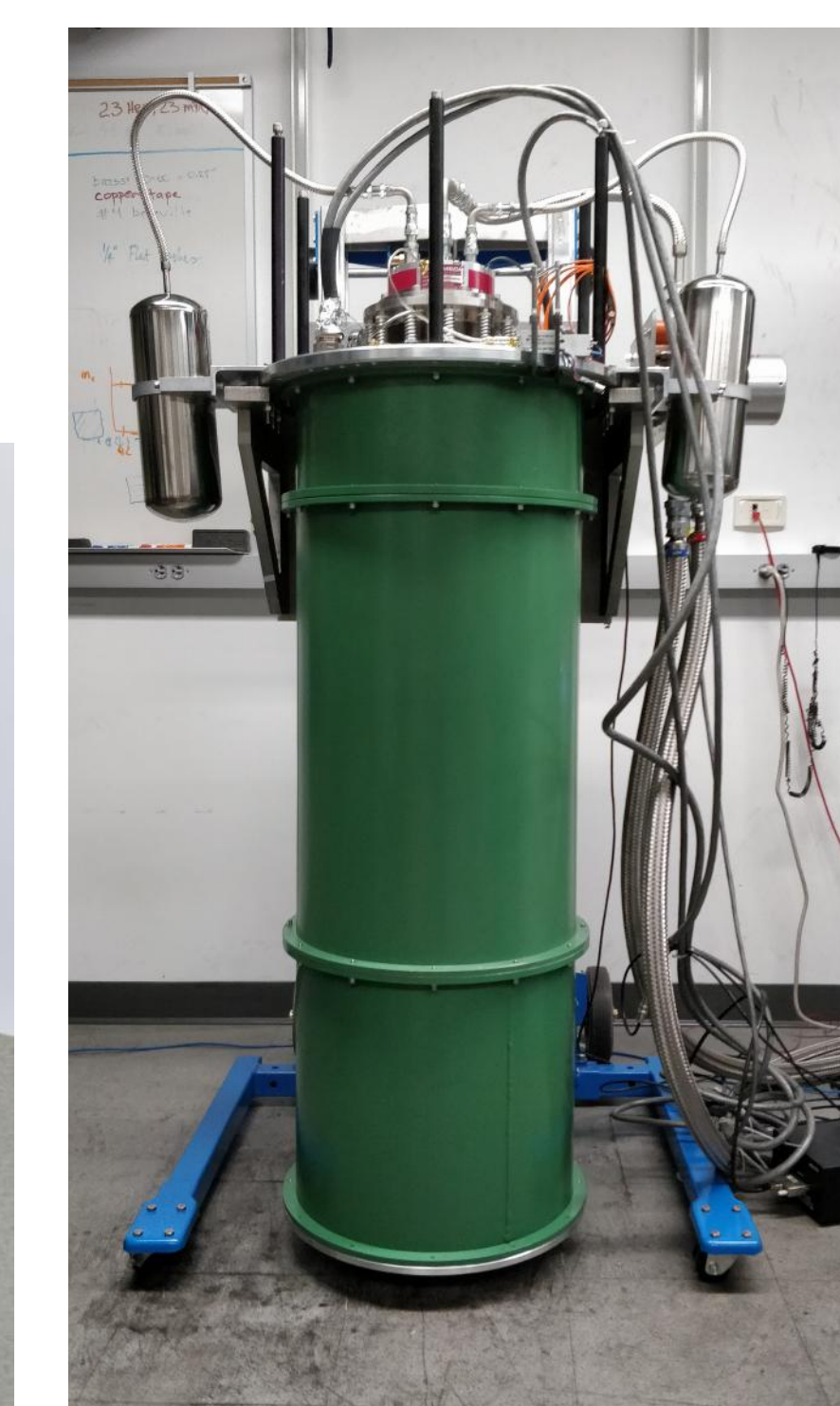
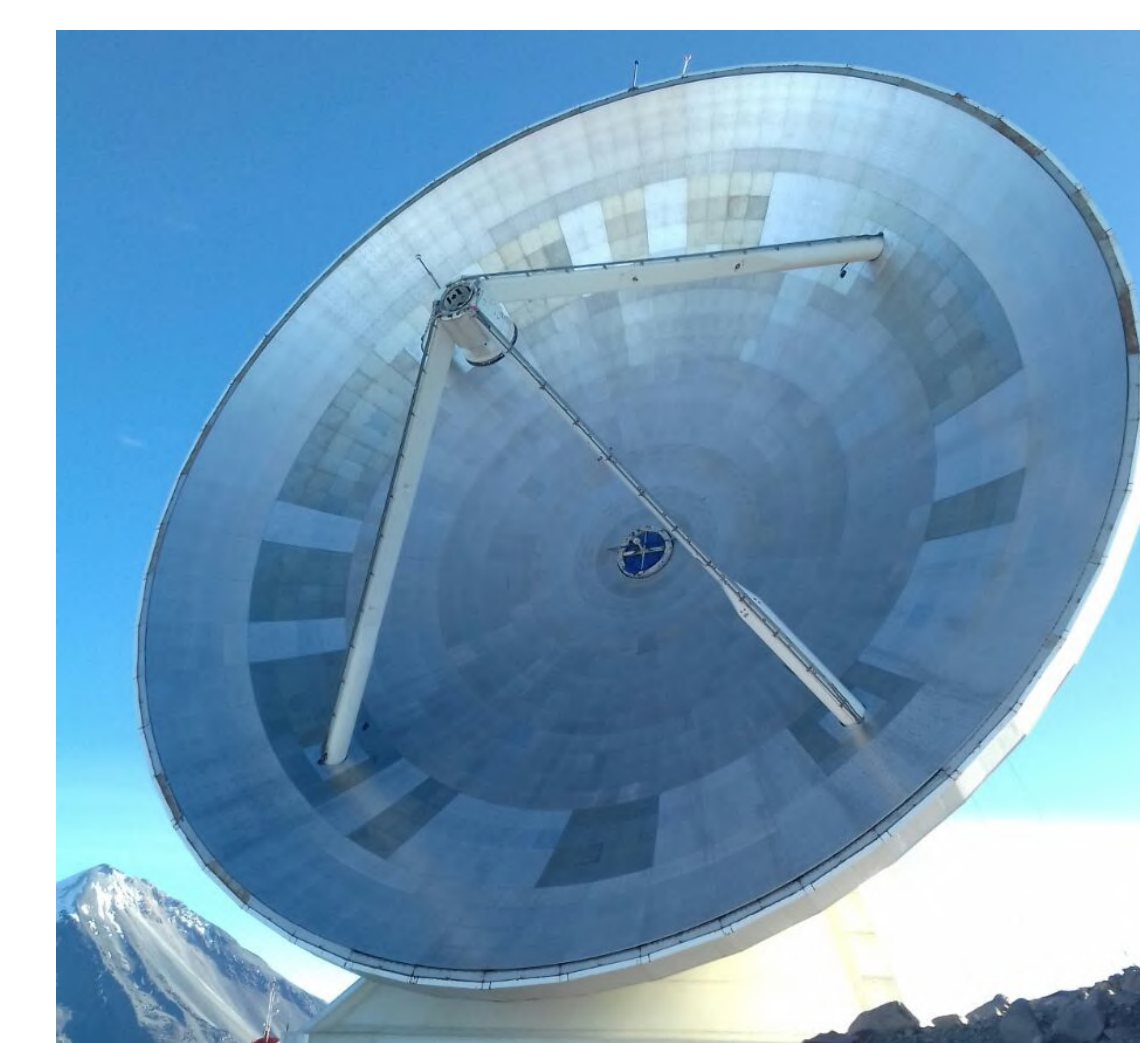


Fig 5: Left The optical coupling of the incident radiation onto the die is done by using a lens coupled antenna. The lens is a Silicon lens mounted on the backside of the die with an AR coating of stycast is applied to the silicon lens to improve optical performance. Right The cold stage with 6 lens mounted devices in the two polarization packages of 3 pixels.

## LOOKING FORWARD

SuperSpec will be deployed on the Large Millimeter Telescope (LMT), a 50m telescope on Volcan Sierra Negra in Mexico. The deployment of SuperSpec on the LMT was delayed by almost a year due to COVID disruptions. But LMT is starting up operations, and SuperSpec plans to be on sky in early 2021. We are currently in the process of preparing the cryostat, mirrors, and readout system to be shipped to the telescope. The demonstration instrument will have three dual-polarization pixels composed of 6 SuperSpec dies. They will be covered with a system of 6 ROACH2 systems with a python control program developed in collaboration with Cardiff, described in more detail in [1]. Erik Shirokoff's talk (11453-15) will focus on the on-sky demonstration and its preparations.



## REFERENCES

1. K. Karkare et al., 2020, JLTP Vol 199
2. P. Madau & M. Dickinson, 2014, ARA&A vol 52
3. G. Che, 2018, ASU Ph.D. Thesis
4. R. McGeehan et al., 2018, JLTP Vol 193